Kashima *et al. J Wood Sci* (2020) 66:27
https://doi.org/10.1186/s10086-020-01874-3

Journal of Wood Science

ORIGINAL ARTICLE

Open Access

Simultaneous detection of density, moisture content and fiber direction of wood by THz time-domain spectroscopy

Moe Kashima, Satoru Tsuchikawa and Tetsuya Inagaki*

Abstract

In the wood product-manufacturing process, the physical properties of wood must be monitored. The terahertz (THz) radiation has a high potential for sensing and imaging wood with a good spatial resolution. This study demonstrates the simultaneous prediction of the density, moisture content, and fiber direction of wood, which are important in determining the wood quality, using THz time-domain spectroscopy. We measured the spectra of 12 kinds of wood at various moisture contents while rotating the sample against the THz wave polarization. The fiber direction was predicted by observing the birefringence, which is the optical property of a material, in which the refractive index depends on the polarization direction. The density and the moisture content were predicted by multiple linear regression using the refractive indices and absorption coefficients obtained from the THz measurement. In a series of THz measurements, we successfully identified the wood fiber direction with an R^2 of 0.90 and a root mean square error (RMSE) of 16.51° (total measured range = 0–170°), the density with an R^2 of 0.97 and an RMSE of 0.022 (total measured range = 0.25–0.67 g/cm^3), and the moisture content with an R^2 of 0.78 and an RMSE of 4.06 (total measured range = 0.00–30.98%).

Keywords: THz time-domain spectroscopy, Density, Moisture content, Fiber direction, Birefringence

Introduction

Wood is a natural material widely used as a building and papermaking material and biomass energy. However, the variations in its material properties can cause serious problems in industrial processes, where uniform raw materials are essential in producing consistent, high-quality products. The wood quality is evaluated by various factors, including density, moisture content (MC), and fiber direction, which greatly influence the wood properties [1]. The most important property of wood is strength. Wood strength is generally estimated from the modulus of elasticity (MOE) in the factory. The MOE of wood can be determined using non-destructive methods, such as static bending [2], stress wave propagation [3], microwave [4], and near infrared [5], with the overall goal of using such techniques for in-line applications. A higher-density wood generally has higher MOE and strength [2]. MC also has a significant effect on strength under the fiber saturation point (FSP). Two kinds of water can be found in a living tree: one is free water, which exists in the lumen or free space in the wood, and the other is bound water, which is held in the amorphous region within the cellulose, hemicellulose, and on the surface crystalline region of the cellulose by hydrogen bonding [6]. Bound water strongly affects the properties of wood below the FSP; hence, the MC must be controlled and monitored [7]. The other important parameter affecting wood strength is fiber direction. Wood is an anisotropic material, with independent mechanical properties in the three directions: longitudinal, radial, and tangential. The difference in the Young's modulus depending on the wood direction is roughly in the L direction:R direction:T direction = 10:1–2:0.5. Thus, measuring the density, MC, and fiber direction without contacting and

*Correspondence: inatetsu@agr.nagoya-u.ac.jp
Graduate School of Bioagricultural Sciences, Nagoya University, Furo-cho, Chikusa-ku, Nagoya 464-8601, Japan

destroying the wood is of importance when sawing wood or designing engineering wood [8].

The terahertz (THz) wave is an electromagnetic wave in the 100 GHz to 10 THz region, which is between microwave and infrared, and can penetrate a wide variety of non-conducting materials, such as paper, wood, masonry, plastic, and ceramics. THz time-domain spectroscopy (THz-TDS) is a spectroscopic technique, in which the properties of matter are probed with short pulses of THz radiation. In this method, the waveform of a THz pulse wave measured after passing through or reflecting in a material is subjected to Fourier transform to obtain the amplitude and phase for each frequency. The complex refractive index of the sample can be obtained by analyzing the amplitude and phase [9]. The refractive index is determined by the physical properties of the material; therefore, the physical properties can be predicted by examining the relationship between the refractive index and the physical property values. This new technology has a high application potential in various industries, including quality control in product manufacturing, security, biosensing, and artwork restoration. THz-TDS also has a potential as a useful tool for the nondestructive investigation of wood. In fact, it has already been shown as a suitable tool for investigating wood (e.g., wood identification [10], imaging of defects in building blocks [11], and dendrochronology [12]). Measurements using THz waves have several advantages. First, the spatial resolution is in sub-millimeter, while the microwave, which has a longer wavelength, is in the order of several centimeters. Second, it is relatively transparent to wood. THz waves have a longer wavelength than visible and infrared rays; thus, the THz wave scattering is less, and it penetrates into the material. Third, the THz radiation is non-ionizing, and poses no significant health concerns, unlike X-rays. Fourth, the complex refractive index values can be obtained by THz-TDS although only the absorbance information can be obtained for visible, near infrared (NIR), infrared (IR) or X-ray spectroscopy because of high frequency.

Some studies have reported on the evaluation of three physical property values, that is, density, MC, and fiber direction [9, 13–17]. Reid et al. [9] found that solid wood is shown to exhibit both strong birefringence and diattenuation in THz regions. Todoruk et al. [18] concluded that the large birefringence observed may be due to either intrinsic or form birefringence, although the source of birefringence varies according to species, the trend shows contributions from both types of birefringence. It is expected that one can determine the wood fiber direction by observing the change of index refraction value as a function of angle between THz polarization and wood grain angle as Reid et al. [9] predicted the fiber direction of lens paper. Although some researches reported the prediction of fiber direction for THz signal, these used any kind of fiber-integrated samples which have the same complex refractive index. In the actual measurement in wood product factory, wood samples have wide range of complex refractive index values changing with the density and the MC of wood. There have been no research reporting the fiber direction prediction for the sample which have wide variations of complex refractive index values. Inagaki et al. [17] successfully performed a simultaneous prediction of density and MC. After THz measurements of wood at various MCs were taken for two orientations of the THz field (parallel and perpendicular) with respect to the visible grain, they extend a model that has been applied previously to oven-dry wood [14] to include the effects of moisture below the fiber saturation point by combining two effective medium models, which allows the dielectric function of water, air and oven-dry cell wall material to be modeled to give an effective dielectric function for the wood. The complex refractive index values of wood are a function of fiber direction, density and MC. The present study is based on previous studies and showed a simultaneous prediction of the fiber direction, density, and water content. We tried to extract the fiber direction, density and MC of wood samples from the complex refractive values measured at four different orientation angles between THz polarization and fiber direction of wood. The experiment was demonstrated through a series of THz measurements using 12 kinds of wood species below the FSP. Wood exhibits a strong birefringence; therefore, the fiber direction was predicted herein by measuring the change in the refractive index while rotating the wood. The density and MC were predicted by investigating the relationship among the obtained refractive index, absorption coefficient, density, and MC.

Materials and methods

Sample preparation

Twelve kinds of species were investigated to exhibit a big variation in density (Table 1). The samples were cut from radial and tangential planes. Some samples between these two planes were roughly 3 mm thick and 20×20 mm^2.

THz-TDS measurement

Polarized THz transmission spectroscopy was performed using a Tera Prospector-Kit model (NIPPO PRECISION, Nirasaki, Japan). The bandwidth extended from approximately 0.01 to 4.00 THz. The THz beam spot diameter at the sample was approximately 5 mm. The detection of the THz wave is a component in the same direction as the polarization direction of the incident THz wave. The reference measurements without the sample were taken

Table 1 Properties of the wood samples

Common name	Botanical name	Oven-dry density (g/cm^3)	Oven-dry thickness (mm)
Agathis	*Agathis alba Foxw*	0.38	2.68
Ayous	*Triplochiton scleroxylon*	0.37	2.11
Araucaria	*Araucaria heterophylla*	0.41	2.08
Yellow poplar	*Liriodendron tulipifera*	0.51	2.86
Princess tree	*Paulownia tomentosa*	0.25	2.62
Rubber tree	*Hevea brasiliensis*	0.63	2.67
Japanese cedar	*Cryptomeria japonica*	0.36	2.70
Caster aralia	*Kalopanax pictus*	0.55	2.67
Japanese ash	*Fraxinus mandshurica*	0.62	2.76
Japanese cypress	*Chamaecyparis obtusa*	0.40	2.76
Red cedar	*Thuja plicata*	0.34	2.76
European beech	*Fagus sylvatica*	0.64	2.83

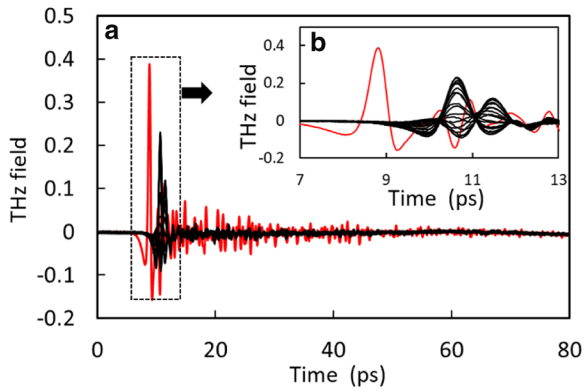

Fig. 1 **a** Reference (red line) and measured THz wave forms passing through the 2.76-mm-thick oven-dry sample of Japanese cypress. **b** Enlarged view

before and after each THz measurement set and the average values were used for analysis.

Measurement procedure

First, the wood samples were dried in a convection oven for 48 h at 103 °C and used for THz measurement. Before and after the THz measurements, the samples were weighed (±0.0001 g) and the average weight values were used for calculation of MC. The sample dimensions (length, width, and thickness) were measured using calipers (±0.01 mm) before all the THz measurements. After the THz measurement of the oven-dry wood, the samples were conditioned at different relative humidities (RH) to obtain different MC. The samples were then placed in a humidity-conditioned desiccator and left for at least 48 h to ensure that they reach an equilibrium MC. Humidity was adjusted by changing the concentration of H_2SO_4 solutions. The THz measurement was repeated by changing the MC step by step (RH = 65, 85, 95, 100%). This process was repeated for each MC, progressing from a low to high MC. THz measurements were conducted under room condition at the temperature of 26 °C. Although there are strong absorptions due to water vapor at 0.56, 0.75, 0.99 THz (below 1 THz), we confirmed that there were no significant changes in these absorptions for the reference THz measurement before and after the sample THz measurement. The maximum changes in the MC of wood samples before and after the THz measurements were 0.022, 0.24, 0.73, 1.23 and 2.62% when the RH was oven-dried, 65, 85, 95 and 100%, respectively.

The THz time-domain spectroscopic measurement was performed for each sample and each orientation of the polarization with respect to the visible grain. The time-domain waves were collected for the different THz polarization orientations with respect to the grain by rotating the wood sample (from 0° to 180° in 10° increments).

Data analysis

The densities (ρ) and the MC were calculated as follows:

$$\rho = \frac{W}{V}, \tag{1}$$

$$\mathrm{MC} = \frac{\rho_{\mathrm{wetwood}} - \rho_{\mathrm{drywood}}}{\rho_{\mathrm{drywood}}} \times 100(\%), \tag{2}$$

where W is the weight of wood; V is the volume of wood calculated from the physical dimensions; and ρ_{wetwood} and ρ_{drywood} are the density of the wet and oven-dry wood, respectively. Table 1 shows the determined oven-dry density and thickness.

The phase and the amplitude spectrum were obtained through the Fourier transformation of the measured time-domain waveform (Fig. 1). The refractive index n and the absorption coefficient α were obtained using the following equations:

$$n = -\frac{\varphi c}{2\pi \nu d} + 1, \tag{3}$$

$$\alpha = -\frac{2}{d}\ln\left(\frac{E(n+1)^2}{4n}\right), \tag{4}$$

where φ is the phase difference between the reference and sample measurements; c is the speed of light in vacuum; ν is the frequency; d is the sample thickness; and E is the amplitude spectrum.

The refractive index and the absorption coefficients were determined and averaged over the frequency range

of 0.30 to 0.35 THz. We used the frequency range of 0.30–0.35 THz because (1) THz intensity acquired with the measurement system is high in this range; (2) calculated index refraction values in this range were identical with frequency; (3) in order to minimize the effect of absorption of water vapor found at 0.56, 0.75 and 0.99 THz.

Results and discussion

The fiber direction can be predicted by observing the birefringence, which is the optical property of a material with a refractive index that depends on the polarization and the propagation direction. According to Reid et al. [9], wood exhibits high birefringence and diattenuation in the THz region. The birefringence in wood has two origins. The intrinsic birefringence is found in crystalline materials (cellulose crystalline region in wood), and the observed birefringence characteristics can be explained in terms of the dielectric properties of the molecules that make up the crystal. The form birefringence can occur on a much larger scale and when an array of ordered particles (cell wall array), which are large compared to the molecule size, but small compared to the light wavelength, exists. All the samples in this study were matured wood; hence, their microfibril angles are expected to be close to 0°, and the main origin of the measured birefringence is expected to be the form birefringence (wood fiber direction). Birefringence can be observed from the phase shift between the orthogonal polarization components and a corresponding propagation delay in the time domain. Figure 1 shows typical time signals rotating the wood samples with respect to the THz polarization. The THz field polarized perpendicular (⊥) with respect to the visible grain arrived first, while that polarized parallel (∥) arrived last. We calculated the refractive index and absorption coefficient values from the time-domain signal using Eqs. (3) and (4) and averaged them between 0.30 and 0.35 THz. The fiber direction of the wood samples can be estimated by observing the index refraction values. Jordens et al. [19] showed that the THz measurements at the same spatial position with more than three differing orientation angles of the THz polarization with respect to the edge of the sample must be performed to identify the direction angle. They used three differing direction angles of the THz polarization because the refractive index and absorption values were almost identical for all the samples. However, we employed four different direction angles to predict the fiber direction of the wood samples, because the prediction of fiber orientation and MC and density was not stable when we employed only three different direction angles for the fitting like Jorderns et al. The reason why the prediction was bad when using three different direction angles is that the variations in the refractive index and absorption coefficient acquired in this study were significantly bigger compared to their result due to big variations of MC and density. The refractive index can be simply given by the following equation according to Jordens et al. [19]:

$$n_\theta = \left(\cos^2\theta\right) n_\parallel + \left(\sin^2\theta\right) n_\perp. \tag{5}$$

Hence, we determined the best n_θ, $n_\parallel$, and $n_\perp$ with the minimum error values between the estimated value from Eq. (5) and the measured values at four difference direction angles (i.e., n_θ, $n_{\theta+\beta}$, $n_{\theta+2\beta}$, and $n_{\theta+3\beta}$, where $n_\parallel$ and $n_\perp$ are the refractive indices with the THz polarized parallel and perpendicular with respect to the visible grain, respectively; θ is the angle between the wood grain and the THz wave polarization; and β is the interval angle). We tried all combinations of θ and β and calculated the determination coefficient value between the predicted and measured θ, where 50° gave the best prediction result for the fiber grain angle θ, $n_\parallel$ and $n_\perp$. We got almost the same prediction accuracy when we applied $\beta = 40°$. This result is consistent with the previous study [19] which stated that the accuracy was highest when the interval was 45°. The reason for the good prediction with $\beta = 40°$ is because the wide range of variation in the measured n at four difference direction angles can be used for fitting with Eq. (5). For example, the variation of n in four difference direction angles would be relatively small compared to the variation between $n_\parallel$ to $n_\perp$ when we applied $\beta = 10°$. Also, the variation of n in four difference direction angles would be small when β is too large (i.e., when $\beta = 90°$, the n value used for the fitting would be n_θ, $n_{\theta+90°}$, $n_{\theta+180°}$, and $n_{\theta+270°}$, where the value of n_θ and $n_{\theta+180°}$ are almost identical). Figure 2a shows the representative relation between the directions of the THz field with respect to the visible grain and the refractive index of oven-dried Japanese Ash (density = 0.62 g/cm^3). The black filled circles in the figure denote the measured refractive index values. The solid lines represent the estimated value from Eq. (5) by the estimation of n_θ, $n_\parallel$, and $n_\perp$ from $n_{10°}$, $n_{60°}$, $n_{110°}$, and $n_{160°}$, which are shown as red filled circles (in this example, $\theta = 10°$ and $\beta = 50°$). The change of the refractive index values can be well predicted from four kinds of refractive index values. The relationship between the measured and predicted angles θ for all species at all the MC was good with a determination coefficient value of $R^2 = 0.90$ and a root mean square error (RMSE) value of 16.51° (Table 2). Determination coefficient value and RMSE were calculated using:

$$R^2 = 1 - \frac{\sum \left(y - y_{\text{pred}}\right)^2}{\sum \left(y - \bar{y}\right)^2}, \tag{6}$$

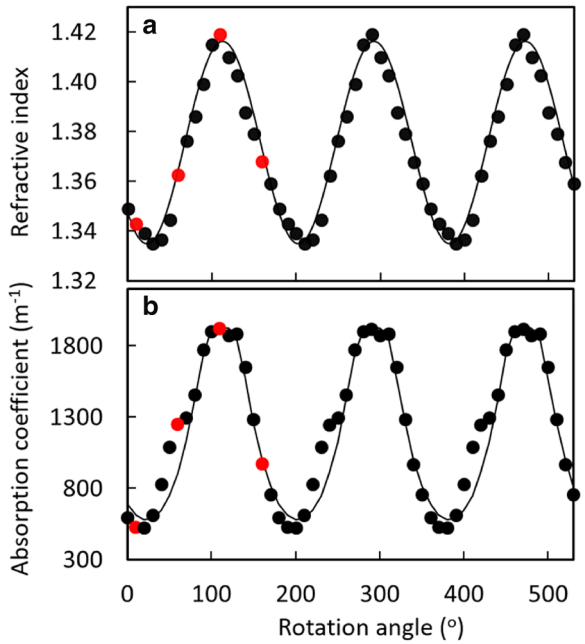

Fig. 2 Relationship between the rotation angle and the measured **a** refractive index and **b** absorption coefficient (circles) and simulated values (solid line) of oven-dried Japanese ash (density = 0.62 g/cm^3). The data used for the prediction are shown by the red circles

$$\mathrm{RMSE} = \sqrt{\frac{\sum \left(y - y_{\mathrm{pred}}\right)^2}{n}}, \tag{7}$$

where y is the measured value, y_{pred} is the predicted value, $\bar{y}$ is the average value of measured value and n is the number of samples.

The equation for the THz transmission intensity E is presented as follows according to [9]:

$$E = a\sqrt{\cos^4\theta \exp\left(-\alpha_\perp d\right) + \sin^4\theta \exp\left(-\alpha_\parallel d\right) + 2\sin^2\theta\cos^2\theta\left(\Gamma_\perp + \Gamma_\parallel\right)\exp\left(-\frac{\left(\alpha_\perp + \alpha_\parallel\right)d}{2}\right)}, \tag{8}$$

where a is a coefficient, and $\Gamma_\parallel$ and $\Gamma_\perp$ are the phase retardances incurred parallel and perpendicular to the grain, respectively ($\Gamma = 2\pi nfd/c$). The transmitted THz intensity from wood can be expressed with, θ, phase retardances calculated from $n_\parallel$ and $n_\perp$, and $\alpha_\perp$ and $\alpha_\parallel$ as Eq. (8). By using θ, $n_\parallel$ and $n_\perp$ calculated from Eq. (5), we determined the best a, $\alpha_\perp$ and $\alpha_\parallel$ with the minimum error values between the estimated value from Eq. (8) and the measured values at four difference direction angles (i.e., E_θ, $E_{\theta+\beta}$, $E_{\theta+2\beta}$, and $E_{\theta+3\beta}$). Figure 2b shows the relationship between the directions of the absorption coefficient with respect to the visible grain. As explained above, the $n_\parallel$, $n_\perp$ and θ (angle between THz polarization and fiber orientation) were estimated by fitting refractive index values measured at four difference direction angles to Eq. (5) at first, then $\alpha_\perp$ and $\alpha_\parallel$ were estimated by fitting the measured THz transmission intensity at four difference direction angles to Eq. (8) using the determined $n_\parallel$, $n_\perp$ and θ. Although it should be pointed out that Eq. (5) does not take into account the effect of extinction of THz wave, we employed the procedure to estimate $n_\parallel$, $n_\perp$, $\alpha_\perp$, $\alpha_\parallel$ and θ from n and THz transmission intensity measured at four difference direction angles, because the estimated $n_\parallel$, $n_\perp$, $\alpha_\perp$, $\alpha_\parallel$ were almost the same as the actually measured values.

Figure 3 depicts the dependence of the estimated $n_\parallel$ and $\alpha_\parallel$ with wood density and MC, where the regression lines were drawn for each species. For each species, both the refractive index and the absorption coefficient had strong correlations with both the density and the MC. The range of determination coefficients between $n_\parallel$ and density, $n_\parallel$ and MC, $\alpha_\parallel$ and density, and $\alpha_\parallel$ and MC for each species was 0.80–0.998, 0.65–0.97, 0.73–0.99, and 0.59–0.98, respectively. These strong correlations suggest the possibility of a simultaneous prediction of both quantities from the measured THz signal. Inagaki et al. extended a model, including the effects of moisture below the FSP by combining two effective medium models, which allowed the dielectric function of water, air, and oven-dry cell wall material to be modeled to give an effective dielectric function for the wood and showed a strong correlation between the measured and predicted values of density

Table 2 Result of the prediction of the density, moisture content, and fiber angle when the interval angle is 50°

	Range of the measured data	Standard deviation of the measured data	R^2	RMSE
Density	0.25–0.67 (g/cm^3)	0.12 (g/cm^3)	0.97	0.022 (g/cm^3)
Moisture content	0.00–30.98 (%)	8.89 (%)	0.78	4.06 (%)
Fiber direction	0–170 (°)	51.91 (°)	0.90	16.51 (°)

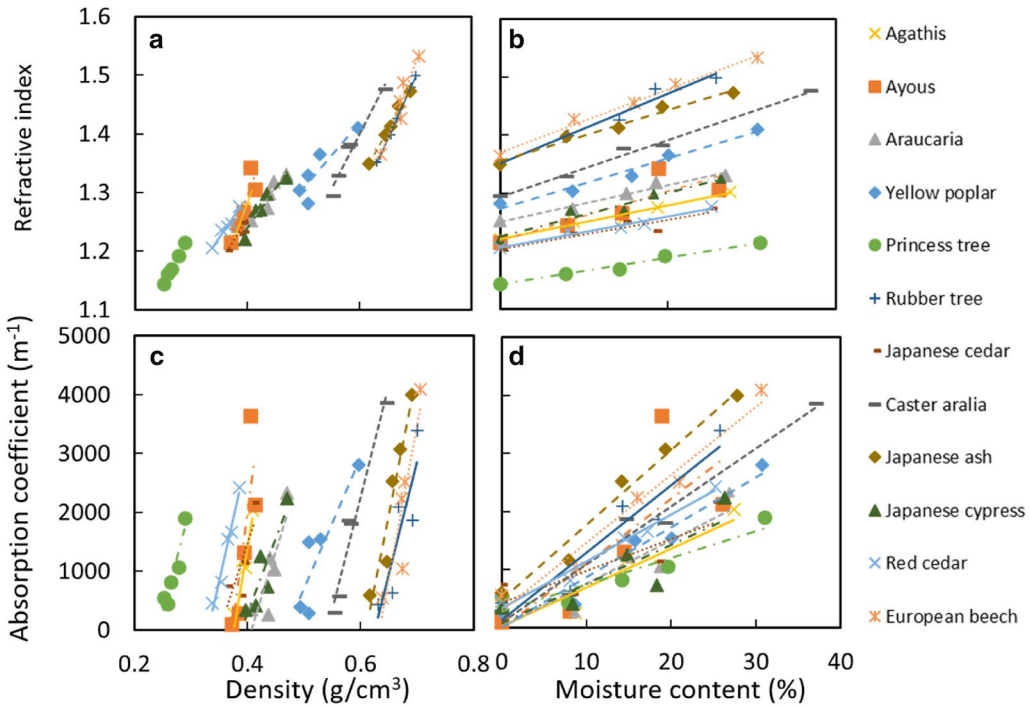

Fig. 3 Relationship between the refractive index and the **a** density, **b** moisture content and absorption coefficient, **c** density, and **d** moisture content. The regression lines are drawn for each sample

and MC. The large scatter between the species in Fig. 3 resulted from the difference of the volume fraction of the cell wall material. Wood is a composite material of air, cell wall material, and water. The volume fraction of the cell wall in the same species is thought to be identical; hence, the change of the refractive index and the absorption coefficient can be well explained by the amount of water if we pay attention to one species. However, considering all wood species, both the amount of water and the volume fraction of the cell wall material were different for each species. Inagaki et al. [17] reported the use of effective medium theory for the prediction of density and MC from the complex permittivity values of wood in THz regions. They regarded wood as a composite mixture of oven-dry wood cell wall, water and air. They extracted the volume fraction of each component from measured permittivity of wood after they decided the permittivity of each of the components in advance. As these methods are generally based on the linear relation between permittivity of wood and volume fraction of oven-dry wood cell wall, water and air, we simply and directly predicted the MC and density from measured permittivity or complex refractive index (in this study, we used real part of refractive index value and absorption coefficient) using multiple linear regression (MLR). As the prediction results from permittivity and real part of refractive index value and absorption coefficient were almost the same, the prediction result from real part of refractive index value and absorption coefficient were explained in this manuscript. The MLR was performed using $n_{\parallel}$, $n_{\perp}$, $\alpha_{\parallel}$, and $\alpha_{\perp}$ to predict the density and MC as the objective variables. Table 2 shows the results of predicting the density, MC, and fiber angle with an interval angle β of 50°. It exhibited good prediction, with determination coefficient values of $R^2 = 0.97$ and 0.78 and RMSE values of 0.022 g/cm^3 and 4.06% for density and MC, respectively. Determination coefficient value and RMSE were calculated using Eqs. (6) and (7). The methods worked for various kinds of wood, including both softwood and hardwood, in which the structural differences are significant.

The three parameters (i.e., fiber direction, density, and MC) can also be simultaneously determined at microwave frequencies. Schajer and Orhan [19] successfully predicted the grain angles for hemlock and Douglas fir with standard errors of 0.9° and 2.5° (measured range from −90 to +90°), MC of 1.2 and 1.9% (measured range from 7 to 28%), and dry density of 0.16 and 0.30 g/cm^3 (measured range from 0.325 to 0.625 g/cm^3) [20]. Liang et al. [20] exhibited an acceptable predictive performance by using NIR spectroscopy for the MC with a determination coefficient of 0.98 and a standard error of prediction of 2.51% and basic density with a determination

coefficient of 0.87 and a standard error of prediction 17.61 kg/m^3 [21]. In order to examine the source of error for the prediction of fiber direction and MC, we observed the prediction accuracy change with the MC of wood. Figure 4a shows the relationship between the reference values of angle between fiber direction and THz orientation, and predicted value from THz signal (RH = 85%). We calculated intercept and correlation coefficient from the regression line between them (i.e., intercept is −4.28 and correlation coefficient is 0.99 for RH = 85%) for all the TH levels (0, 65, 85, 95 and 100%). Figure 4b shows the relation between RH and calculated the absolute value of intercept and correlation coefficient. The intercept value tends to be high at low RH (i.e., the predicted values are overestimated at low RH). Todoruk [18] shows the birefringence increase with MC of wood. We consider that not only the birefringence value, but also properties like axial direction of birefringence would change with MC result overestimation of angle at lower RH values. In contrast, correlation coefficient value between them decreased when RH increased. This is attributed to the low transmission intensity of THz wave from the high-MC wood samples. The density prediction was good even in the high RH because the effect of low intensity of THz wave (i.e., signal-to-noise ratio) on the real part of refractive index value, which is strongly related to the density of wood, is not the significant. However, the signal-to-noise ratio directly affects the absorption coefficient result in the worst prediction of MC. Although the prediction accuracy was not better than the other wavelength ranges, the THz region has an advantage for the spatial resolution compared to the microwave region and transparency compared to the NIR regions. We considered it best to use the THz electromagnetic wave for the evaluation of engineering wood (i.e., laminated wood, plywood, and oriented strand board), because of the transparency and spatial resolution of THz and the thickness and low MC of engineering wood, although the best application of the microwave angle might be the evaluation of a bigger size of wood (i.e., log and timber).

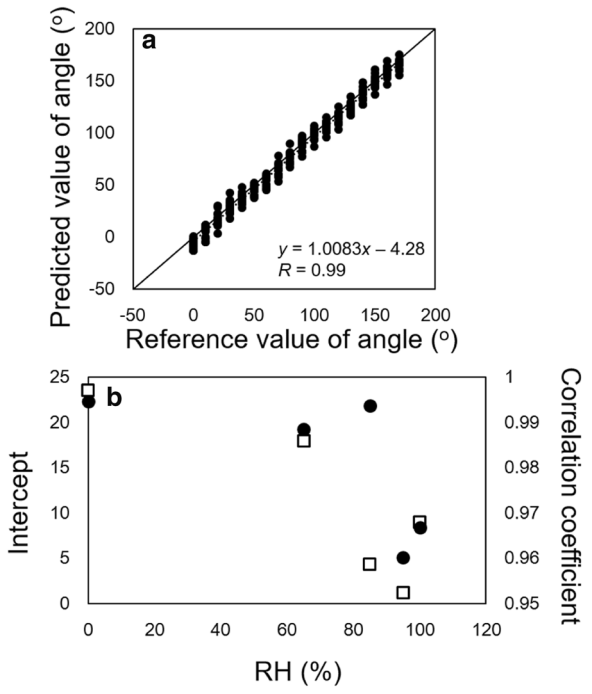

Fig. 4 **a** Relationship between the reference values of angle between fiber direction and THz orientation, and predicted value from THz signal (RH = 85%). **b** Relation between relative humidity and intercept (opened square) and correlation coefficient (closed circle) of regression line between reference values of angle between fiber direction and THz orientation

Conclusion

The fiber direction, density, and MC of the 12 species of wood were simultaneously estimated by THz time-domain spectroscopy. The refractive index and the absorption coefficient had a strong correlation with the density and MC. The MLR model based on the values of $n_{\parallel}$, $n_{\perp}$, $\alpha_{\parallel}$, and $\alpha_{\perp}$ performed a good prediction of the density with an R^2 of 0.97 and an RMSE of 0.022 (total measured range = 0.25–0.67 g/cm^3) and of the MC with an R^2 of 0.78 and an RMSE of 4.06 (total measured range = 0.00–30.98%). The values of the refractive index and the absorption coefficient changed according to the rotation angle of the sample because of the wood birefringence. Measuring under four differing rotation angles of the sample enables us to determine the fiber direction with an R^2 of 0.90 and an RMSE of 16.51°. Our results demonstrated that THz time-domain spectroscopy is an appropriate method for the non-destructive testing of wood.

Abbreviations

FSP: Fiber saturation point; IR: Infrared; MOE: Modulus of elasticity; MC: Moisture content; MLR: Multiple linear regression; NIR: Near infrared; RH: Relative humidity; RMSE: Root mean square error; THz: Terahertz; THz-TDS: THz time-domain spectroscopy.

Acknowledgements

Not applicable.

Authors' contributions

MK did the experiments, analysis and manuscript writings. ST gave suggestions about the analysis. TI organized the research. All authors read and approve the final manuscripts.

Funding

This work was supported by JSPS KAKENHI Grant Number JP 16H02559.

Availability of data and materials

The datasets used and analyzed during the current study are available from the corresponding author on reasonable request.

Competing interests
The author declare that they have no competing interests.

Received: 21 November 2019 Accepted: 2 April 2020
Published online: 10 April 2020

References

1. Beall FC (2000) Subsurface sensing of properties and defects in wood and wood products. Subsurf Sens Technol Appl 1:181–204
2. Shmulsky R, Jones PD (2011) Forest products and wood science; an introduction, 6th edn. Wiley-Blackwell, Hoboken
3. Edlund J, Lindstrom H, Nilsson F, Reale M (2006) Modulus of elasticity of Norway spruce saw logs vs. structural lumber grade. Holz Als Roh-Und Werkst 64:273–279
4. Lundgren N, Brannstrom M, Hagman O, Oja J (2007) Predicting the strength of Norway spruce by microwave scanning: a comparison with other scanning techniques. Wood Fiber Sci 39:167–172
5. Via B, So C-L, Shupe T, Eckhardt L, Stine M, Groom L (2005) Prediction of wood mechanical and chemical properties in the presence and absence of blue stain using two near infrared instruments. J Near Infrared Spectrosc 13:201–212
6. Skaar C (1988) Wood-water relations. Springer, Berlin
7. Hartley ID, Kamke FA, Peemoeller H (1992) Cluster theory for water sorption in wood. Wood Sci Technol 26:83–99
8. Forest Products L (1999) Wood handbook: wood as an engineering material. Forest Products Laboratory, Madison
9. Reid M, Fedosejevs R (2006) Terahertz birefringence and attenuation properties of wood and paper. Appl Opt 45:2766–2772
10. Wang Y, She S, Zhou N, Zhang J, Yan H, Li W (2019) Wood species identification using terahertz time-domain spectroscopy. BioResources 14:1033–1048
11. Oyama Y, Zhen L, Tanabe T, Kagaya M (2009) Sub-terahertz imaging of defects in building blocks. Ndt E Int 42:28–33
12. Jackson JB, Mourou M, Labaune J, Whitaker JF, Duling IN, Williamson SL, Lavier C, Menu M, Mourou GA (2009) Terahertz pulse imaging for tree-ring analysis: a preliminary study for dendrochronology applications. Meas Sci Technol 20:075502
13. Koch M, Hunsche S, Schuacher P, Nuss MC, Feldmann J, Fromm J (1998) THz-imaging: a new method for density mapping of wood. Wood Sci Technol 32:421–427
14. Inagaki T, Hartley ID, Tsuchikawa S, Reid M (2014) Prediction of oven-dry density of wood by time-domain terahertz spectroscopy. Holzforschung 68:61–68
15. Tanaka S, Shiraga K, Okumura S, Fujii Y, Ogawa Y (2014) Applicability of effective medium theory to wood density measurements using terahertz time-domain spectroscopy. J Wood Sci 60:111–116
16. Zolliker P, Ruggeberg M, Valzania L, Hack E (2017) Extracting wood properties from structured thz spectra: birefringence and water content. IEEE Trans Terahertz Sci Technol 7:722–731
17. Inagaki T, Ahmed B, Hartley ID, Tsuchikawa S, Reid M (2014) Simultaneous prediction of density and moisture content of wood by terahertz time domain spectroscopy. J Infrared Millim Terahertz Waves 35:949–961
18. Todoruk TM, Hartley ID, Reid ME (2012) Origin of birefringence in wood at terahertz frequencies. IEEE Trans Terahertz Sci Technol 2:123–130
19. Jordens C, Scheller M, Wietzke S, Romeike D, Jansen CP, Zentgraf T, Wiesauer K, Reisecker V, Koch M (2010) Terahertz spectroscopy to study the orientation of glass fibres in reinforced plastics. Compos Sci Technol 70:472–477
20. Schajer GS, Orhan FB (2006) Measurement of wood grain angle, moisture content and density using microwaves. Holz Als Roh-Und Werkst 64:483–490
21. Liang L, Fang G, Deng Y, Xiong Z, Wu T (2019) Determination of moisture content and basic density of poplar wood chips under various moisture conditions by near-infrared spectroscopy. For Sci 65:548–555

Publisher's Note